International Journal of Recent Technology and Engineering (IJRTE)
ISSN: 2277-3878, Volume-8 Issue-5, January 2020

The Influence of Elevated Brain Temperature on Intracranial Pressure during Exposure of RF Energy

Kavita Goyal, Moin Uddin

Abstract: ***Brain temperature (BT) and intracranial pressure (ICP) are crucial parameters in precise management of brain rejuvenation in the event of brain injury. In order to reduce medical costs and improve therapeutic effects, it is important to know that the dynamics of BT and ICP are affected due to various reasons. RF energy is also one of the major reason to increase the BT and ICP. In this work, a simple compartment based simulation model has been developed for coupling between RF energy and ICP, with an intention to improve the comprehension of ICP. The model incorporates the cardiovascular output, hemodynamic of cerebral arterial-arteriolar bed, oxygen, and carbon dioxide exchange mechanism between brain tissue and capillary, a non-linear pressure-volume relationship of subarachnoid space. It simulates the interaction between BT, the cerebral metabolic rate of oxygen ($CMRO_2$), a concentration of bicarbonate ions (HCO_3^-), cerebral blood flow (CBF), cerebral blood volume (CBV) and ICP. The basic concept behind the model is the expansion or contraction of brain tissue which is affected underexposure of RF energy. The simulation results determine the following: 1) ICP becomes unstable underexposure of RF energy at higher specific absorption rate (SAR). 2) ICP and brain temperature has a direct relation during exposure of RF energy. The model elaborates the dynamics of ICP with less complexity.***

Keywords: ***Intracranial pressure, brain temperature, RF energy, cerebral metabolism, cerebral blood volume, cell phone***

I. INTRODUCTION

A. Background

The cell phone innovation, one of the most developing advances in the world, has turned into a prominent part of everyday life. Inferable from the electromechanical progressions, noteworthy enhancements have been accomplished in the web information speed. Due to technological revolution, correspondence advancements viz. Wi-Fi, Bluetooth, and 4G have been created. As the correspondence frameworks are moving towards more and more cost effectiveness, individuals invest a large portion of their energy with their cell phones. Consequently, the conceivable unsafe impacts of radio frequency radiation have turned into a worry for individuals (Hardell et al., 2009).

There are several examinations announcing that radio frequency waves discharged by cell phones may cause numerous unsafe consequences for the cellular and molecular dimension viz. DNA harm, distinctive sorts of malignancy, oxidative pressure, lipid peroxidation, increment of free radicals, DNA breaks in the mind, and irregularities in chromosomes (Akdag et al., 2016, 2018; Cam et al., 2012; Chauhana et al., 2017; Dasdag et al., 2015; Deshmukh et al., 2013; Bioinitiative Report 2012; Megha et al., 2015). The impacts of radio frequency and very low-frequency electromagnetic field on blood-brain barrier have been additionally underlined by (Nittby, Grafström, Eberhardt, et al., 2008).

Due to ill effects of electromagnetic radiations on human health as observed in the state of art, the present work tend to move in the direction of finding and evaluating the relationship of changes in neurological parameters with RF energy exposure. During the course of current work, a model has been developed to depict the influence of RF energy on intracranial pressure with the help of available data of brain temperature (Kodera, Tames & Hirata, 2018) during exposure of RF energy. The data of brain temperature at a 3GHz frequency with different SAR has been used in this model. The model calculates the cerebral metabolic rate of oxygen at different values of brain temperature. It estimates the produced amount of CO_2 in terms of bicarbonate ions during metabolic activity. CO_2 serves as one of the fundamental regulators of CBF. The variation in CO_2 results in the changes in CBF as well as CBV. In other terms, any change in CBV will affect the cerebral subarachnoid space, where CSF is absorbed. The modeling results depicted how much temporal changes have occurred in ICP, CBV, and concentration of bicarbonate ions during exposure of the RF energy. It shows the strong interactions amongst exposed RF energy, brain temperature, $CMRO_2$, CBV, and ICP. To the best of our knowledge, no such relationship has established between ICP and temperature of brain exposed under RF energy, by previous studies. Although studies have been found where, in case of head injuries, ICP correlates with brain temperature. The aim of this work is to provide an improvement in thorough understanding of ICP dynamics and brain temperature during RF energy exposure. The simplifications of this introduced simulation model have been clearly presented in a qualitative model description. Its

Manuscript published on January 30, 2020.
* Correspondence Author
Kavita Goyal*, ECE department, Apeejay Stya University, Gurugram, India. Email: jindalkavita82@gmail.com
Moin Uddin, School of Engineering & Technology, Apeejay Stya University, Gurugram, India. Email: prof_moin@yahoo.com

limitations are clearly mentioned to maintain a suitable distance from the ill-advised utilization of model.

B. Motivation

The concept of ICP, first proposed by Monro-Kellie (Mokri, 2001) states that the sum of an intracranial volume of the blood, brain, CSF (cerebrospinal fluid) and other components is constant. An increase in the volume of one component must be compensated by an equal decrease in the volume of another component else there will be an increase in ICP. Many neurosurgical issues are responsible for changes in the intracranial pressure, for example, cerebrum damage (Gowers, 1886), hydrocephalus (Geocadin, Varelas, Rigamonti & Williams, 2007), brain tumour (Petersen, Landsfeldt, Cold, et al., 2003) and intracranial hemorrhage (Hamani, Zanetti, Pinto, et al., 2003). It has also been observed that the increase in ICP is due to changes in blood flow in the brain (Ganong, 1995). The brain can bear with ICH (intracranial hypertension) to a certain extent, beyond which, a slight increase in cerebral volume shows a sharp increase in ICP (Fleisher, Ludwig & Silverman, 2002). A significant cause behind the head injuries and death in pathological conditions is found to be an increase in ICP. The ICP value equal to 20 mmHg is considered as a threshold (Kawoos, Meng & Tofighi, 2015), beyond this limit, it is required to be controlled immediately. It is very important to know all the causes of high ICP for appropriate treatment. Clinically, all such causes of high ICP are well described, but the basic dynamic principle has been less explained.

The purpose of this research is not to interfere with the old causes of high ICP, but to bring forth a new cause which is RF energy. This is an attempt to explore the basic dynamics of ICP with emphasis on how ICP increases when the brain is exposed to RF energy. The intention is to provide significant support for designing better treatment means to control the ICP.

C. Outline

Material and methods section is divided into three parts: The first data acquisition part describes the resources from where the data of brain temperature is collected; part two describes the qualitative simulation model for intracranial pressure dynamics with its assumptions; third part elaborates the investigated changes after exposure of RF energy. Result section elaborates the results of the simulation model. In the discussion section, results have been discussed as well as compared with previously published studies. The research work has been concluded in the conclusion section along with its limitations and future scope.

II. MATERIAL AND METHODS

A. Data acquisition

The concerns have recently been grown for the absorption of radio frequency waves and their devastating effects on human health by increasing the use of mobile phones. In Kodera's experiment (Kodera, Tames & Hirata, 2018), a realistic anatomical human head model TARO (Nagaoka, Watanabe, Sakurai, et al., 2004) was exposed to radiations emitted from a dipole antenna at 300 MHz-10 GHz. Human head model was segmented into skin, fat, muscle, bone and brain like fifty-one anatomical regions. The radiations absorbed by the head model were measured with a specific absorption rate (SAR) in $W.Kg^{-1}$ as defined in Eq. 1. The SAR was calculated with the help of the finite difference time domain (FDTD) method (Taflove & Hagness, 2005). At the same time, the output power of the mobile phone antenna was adjusted so that the average SAR of 10 grams of brain tissue is absorbed in the form of 2 $W.Kg^{-1}$, 10 $W.Kg^{-1}$, 50 $W.Kg^{-1}$, and 100 $W.Kg^{-1}$ as stated in ICNIRP guidelines (ICNIRP, 1998). The penetration depth of the head model due to absorbed radiations is shown in Figure 1a.

$$SAR(r) = \frac{\sigma(r)}{2\rho(r)} |E(r)|^2 \quad (1)$$

Where $|E(r)|$ represents the maximum value of the electric field ($V.m^{-1}$) at position r, symbols ρ and σ and represent the mass density ($kg.m^{-3}$) and conductivity of the brain tissue ($S.m^{-1}$) respectively.

The temperature elevation in the anatomical human head model due to absorbed SAR was calculated with the help of Penne's bio-heat transfer equation (Pennes, 1948) as defined in Eq. 2.

$$C(r)\rho(r)\frac{\partial T(r,t)}{\partial t} = \nabla.\big(K(r)\nabla T(r,t)\big) + \rho(r)SAR(r) + A(r,t) - B(r,t)\big(T(r,t) - T_B(r,t)\big) \quad (2)$$

Where r and t denotes the position vector of tissue and time, $T_B(r, t)$ and $T(r, t)$ denotes the temperature of blood and tissue (°C), K denotes the thermal conductivity of the tissue ($W.m^{-1}.°C^{-1}$), C denotes the specific heat of the tissue ($J.Kg^{-1}.°C^{-1}$), B(r, t) denotes the factor related to blood perfusion ($W.m^{-3}.°C^{-1}$), and A(r, t) denotes the metabolic heat ($W.Kg^{-1}$).

The elevation in brain temperature is represented by Figure 1b at 3GHz and different SAR: 0, 2, 10, 50 and $100W.kg^{-1}$. The temperature of the brain reaches a maximum of 45.5°C at 100 $W.Kg^{-1}$ of SAR. According to Kodera's study, brain temperature reaches its steady state (normal temperature) 37°C within 44 minutes. Data of brain temperature at different SAR has been taken from this study. To synchronization between data of brain temperature and cardiac output, model assumes that brain temperature reaches its steady state within same time as taken by two cardiac cycles. The output of two cardiac cycles has been taken as input in the model.

B. Qualitative description of simulation model

To understand well the changes in the intracranial dynamics under the exposure of

RF energy, a multi-compartment based simulation model has been designed. In the model, blood is taken as an incompressible and sticky fluid which is flowing through the cerebral vasculature.

It distributed into arteries, arterioles, capillaries, veins, and venous sinus. The CSF is produced in the lateral, third and fourth ventricle and absorbed in the spinal cord and surrounding space of brain called cranial subarachnoid space. All compartments are connected as shown in Figure 2. The connectivity of left and right hemispheres of the brain parenchyma with intracranial compartments is depicted in Figure 2.

All compartments, except for the spinal cord, are inside the brain.

The model has been considered for two cardiac cycles as shown in Figure 3a. To initialize the model, it requires the initial amount of blood and its pressure in all compartments which has taken from Linninger research (Linninger, Xenos, Sweetman, et al., 2009). These initial values have been considered as boundary conditions for the model. In each cardiac cycle, blood is pumped out from the heart and delivered to the carotid artery as shown in Figure 3b. The pressure in the carotid artery is shown in Figure 3c. The blood flow is controlled by a pressure difference between the jugular vein and carotid artery. All abbreviations used in Figure 2 are described in Table I. The pressure in artery, arterioles, cranial subarachnoid space and vein are labelled as P_A, P_{AL}, P_{CSAS} and P_V as shown in Figure 3c. Blood flow in artery, arterioles, and vein are labelled as BF_A, BF_{AL} and BF_V as shown in Figure 3d. Also, the produced amount of CSF for two cardiac cycles is depicted in Figure 3d. Other assumptions are presented below to simulate the model:

1. The elasticity of blood vessels which is known as compliance is taken as 2 ml.mmHg^{-1} as per literature (Wang, Ju & Li, 2010).
2. Brain reaches its steady state i.e. 37°C within the same time as taken by two cardiac cycles.
3. Brain temperature is the same as its outer skin temperature.

III. CEREBRAL CHANGES INVESTEGATED DUE TO RF ENERGY EXPOSURE

A. Cerebral metabolism

Elevation in brain temperature at 3GHz with different SAR values is shown in Figure 1b. The increased brain temperature (BT) affects the metabolic rate of oxygen ($CMRO_2$) is well documented in (Greeley, Kern, Ungerleider, et. al., 1991; Thoman, Lampotang, et. al., 1997; Croughwell, Smith, Quill, et. al, 1992) and the mathematical relation between BT and $CMRO_2$ is shown by Eq. 3. In $CMRO_2$ brain tissue consumes the O_2 from capillary and produces the CO_2 as shown in Figure 2. At 37°C, the $CMRO_2$ is calculated to be 3.5 ml.100g^{-1}.min^{-1}, is taken as a steady state value for cerebral metabolism. If brain temperature is shifted up or down from its steady state, the metabolic demand will also shift as per Eq. 3 and also shown in Figure 1c. Table II has discussed the percentage change in $CMRO_2$ on different brain temperatures. It shows that the change in 2°C temperature below its steady state condition has a 20% fall in $CMRO_2$ as well as fall in CO_2 production rate. Whereas, the $CMRO_2$ increases 64% drastically with the temperature rises of 4°C above 37°C. As well as, it increases the CO_2 production rate. Furthermore, the CBF varies 1-2 ml.100g^{-1}.min^{-1} for every 1 mmHg change in CO_2 pressure (Mishra, 2002). Similarly, $CMRO_2$ decreases by 34.3% for 4°C fall in BT and increases by 150% for 8°C rise in BT. At 27°C, CBF is roughly half that of the normal value. By 20°C, CBF is about 10% of the normal value. The oxygen consumption by brain tissue relies on the BT.

$$CMRO_2 = e^{a+b*BT} \quad (3)$$

Where a = -2.7579, b = 0.1089 and BT = brain temperature

B. Concentration of bicarbonate ions in venous

The pressure of carbon dioxide (P_{CO2}) is an important regulator of the cerebral circulation. The total CO_2 produced by cerebral metabolism will diffuse into the blood due to its partial pressure gradient (Lumb, 2012; Geers & Gros, 2000; Arthurs & Sudhakar, 2005). It will absorb in oxygenated blood (see Figure 2) and make the bicarbonate ions. As per our mathematical calculations, it is found that the produced CO_2 is 2.75 times more than the consumption of O_2 by brain tissue during cerebral metabolism as shown by Eq. 4. The most CO_2 is transported in the blood plasma as bicarbonate ions. There are two modes of CO_2 diffusion in blood as discussed below:

1. Ten percent of CO_2 gets dissolved in blood plasma which increases the pressure of CO_2 (obeys Henry's law). The model assumes that the solubility coefficient of CO_2 does not vary with temperature.
2. Approximately 90% of CO_2 is transported into red blood cells, out of which 22% make the carbamino compounds by joining reversibly with the non-ionized terminal amino group (-NH2) of blood-borne proteins and release the H^+ and O_2. Five percent of CO_2 gets dissolved in oxygenated blood (HbO_2). The rest 63% CO_2 formed the bicarbonate ions by CO_2 hydration reaction. Fifty-seven percent of bicarbonate ions diffuse out of red blood cells and brings down its concentration gradient. H^+ cannot move across the membrane. H^+ again combines with HbO_2 and releases the O_2. Ninety percent of CO_2 gets absorbed in HbO_2 section as shown in Figure 2.

Total increased concentration of bicarbonate ions due to elevated brain temperature as shown in Figure 1d. It will increase the CO_2 pressure in venous blood ($PvCO_2$) and it is calculated by Eq. 5 (Higgins, 2008), where pH represents the concentration of hydrogen ions in the blood. Pk is constant and its value is 6.1.

$$P\_CO_2\_B_{tissue} = 2.75 * O_2\_C\_B_{tissue} \quad (4)$$

$$pH = Pk + log\left[\frac{HCO3^-}{0.03*PvCO_2}\right] \quad (5)$$

C. Cerebral blood flow (CBF) and cerebral blood volume (CBV)

The blood circulation is more complex in the brain than the other organs of the human body. Any dysfunction in cerebral blood circulation especially in people having high blood pressure may be one of the major factors in the failure of autoregulation. Here CO_2 behaves as a potent vasodilator. As per Grubbjr's study, the increased CO_2 pressure in the

blood becomes a major factor in alteration of CBF and CBV (Grubbjr, Raichle, Eichling & Ter-Pogossian, 1974). The model linked this study with a simulation model to calculate the changes in CBF and CBV by using the Eq. 6 and Eq. 7. The change in CBV is depicted by Figure 4a under the exposure of RF energy at different SAR.

$$CBF = 1.8P_{CO_2} - 16.75 \quad (6)$$

$$CBV = 0.80\ CBF^{0.38} \quad (7)$$

D. Intracranial Pressure (ICP)

The dynamics of ICP can be better understood if the brain is treated as a 'closed box' or a fixed rigid skull. The components inside the skull consist of blood (10%, 150 ml), brain (80%, 1400 ml) and cerebrospinal fluid (CSF 10%, 150 ml) (Tameem & Krovvidi, 2013). As per Monro-Kellie, any change in the volume of one of these three components is required to be settled by an equal change in the volume of remaining components otherwise ICP will increase. In adults, the normal value of ICP is up to 20 mmHg (Kawoos, Meng & Tofighi, 2015). The RF energy increases the brain temperature that increases cerebral metabolic demand which consequently increases the CO_2 pressure and CBF. The Increased CBF hinders the venous blood drainage function in the jugular vein. The accumulated blood in venous increase the venous volume consequently it will compress the brain tissue. In this process, the cranial subarachnoid space, where CSF is absorbed, will become less and the pressure will increase. This pressure is termed as intracranial pressure (ICP). The ICP at time t depends upon three factors (Goyal, Uddin & Salwan, 2017): total change in cerebral volume due to blood and CSF (ΔV), an elasticity of blood vessel (K_e), and the initial value of intracranial pressure (ICP (0)) as shown by Eq. 8. For simulation modelling, ICP (0) and K_e have been taken as 10 mmHg and 2 ml.mmHg^{-1}. Figure 4b represents the change in ICP at time t due to change in CBV under the exposure of RF energy at different SAR.

$$ICP(t) = ICP(0)e^{\Delta V k_e} \quad (8)$$

IV. RESULTS

The relation of RF energy, the changes in intracranial dynamics has been analyzed through simulation model as shown in Figure 2. RF energy has been taken at 3GHz with various SAR values as 2, 10, 50, and 100 W.kg^{-1}. From the results, it is observed that there is a direct relationship between intracranial pressure and brain temperature during exposure of RF energy.

The heat absorbed by the brain at 3 GHz is described by specific absorption rate (SAR) as shown in Figure 1a. The absorbed RF energy will increase the brain temperature as depicted in Figure 1b at various SAR levels: 2, 10, 50, and 100 W. Kg^{-1}. The model has been simulated for two cardiac cycles as shown in Figure 3a. The blood pumped out from heart to carotid artery for these two cardiac cycles is shown in Figure 3b. Figure 3c represents the initial pressure in the carotid artery, cerebral artery, cerebral arterioles, cerebral vein, and cranial subarachnoid space. Similarly, blood flow in the cerebral artery, cerebral arterioles, and cerebral vein are depicted in Figure 3d. Also, the amount of CSF flown during these two cardiac cycles is shown in Figure 3d.

The elevated brain temperature will increase the cerebral metabolism. Figure 1c and Table II show the changes in metabolic demand due to a change in the brain temperature at different SAR values. Increased metabolic demand will speed up the process of oxygen extraction from capillaries and production of carbon dioxide. A little amount of CO_2 produced gets dissolved in blood plasma and the rest combines with oxy-haemoglobin to forms the bicarbonate ions. The variations in the concentration of bicarbonate ions in venous blood due to elevated brain temperature are shown in Figure 1d. An increase in bicarbonate ions indicates an increase in CO_2 pressure which in turn increases the CBF. The increase in CBF leads to an increase in CBV as shown in Figure 4a. The increased CBV will compress the brain tissue and decrease the intracranial space responsible for absorption of CSF. CSF will get less space for absorption which in turn increases the pressure that is ICP as shown in Figure 4b. The relationship between ICP and brain temperature underexposure of RF energy is shown in Figure 5. Although the results may vary with individuals, it is thought that these findings have significant potential to play a contributing role in further clinical research of ICP dynamics.

V. DISCUSSION

The present simulation model has analyzed the changes in intracranial dynamics (ICP, the cerebral metabolic rate of oxygen, cerebral blood flow, bicarbonate ions, and cerebral blood volume) due to elevated brain temperature underexposure of RF energy.

In our model, the changes in intracranial pressure have been calculated with different SAR values of 2, 10, 50, and 100 W.kg^{-1} at 3GHz. The impact of RF energy on intracranial pressure is shown in Figure 4b and Figure 5. As per Figure 4b, the ICP increases with an increase in brain temperature. These results are similar to those of the results in Nyholm et al. (Nyholm, Howells, Lewén, et al., 2017). Our work distinguishes from the work in (Nyholm, Howells, Lewén, et al., 2017), that they have evaluated the influence of changes in brain temperature on intracranial pressure in case of traumatic brain injury while we have emphasized the same under the exposure of RF energy. It is pertinent to mention that the individual variations may occur.

Our working hypothesis was that the exposure of the brain under RF energy may lead to increase intracranial pressure. While analyzing the effects of RF energy on ICP with a simulation model, it is important to take into account the complexity of the intracranial dynamics (Ziljstra, 1981) including factors such as the pressure-volume relationship, intracranial compliance, and autoregulation of CBF. To find the changes in intracranial pressure, the concept of tissue compression or expansion has been used in our model. RF energy exposure increases the brain temperature (Kodera, Tames & Hirata, 2018) as shown in Figure 1b, which leads to increase the metabolic demand (Edvinsson, Mackenzie & McCulloch, 1993) as shown in Figure 1c. In cerebral metabolism, brain tissue extracts the oxygen from capillary and release the carbon dioxide as a

waste product. Increased metabolic demand speeds up the process of extraction of oxygen from capillary and as well as increase the produced CO_2. The model calculates the produced amount of CO_2 due to elevated brain temperature. This CO_2, produced by brain tissue, dissolve into the blood. A little amount of it gets dissolved in the blood plasma and the rest get absorbed in oxy-haemoglobin. When oxy-haemoglobin gets combined with CO_2, it releases the bicarbonate ions and oxygen in the blood plasma as per chemical reactions as shown in Figure 2.

Figure 1: (a) plot shows the absorbed radiation at 3GHz by the human head model on different SAR ($W.Kg^{-1}$), (b) plot represents the elevated brain temperature at 3 GHz reaches its steady state within the time taken by two cardiac cycles on different SAR values, (c) plot shows the cerebral metabolic rate of oxygen ($ml.100g^{-1}.min^{-1}$) due to elevated brain temperature on different values of SAR, and (d) plot shows the change in the concentration of bicarbonate ions due to the change in the cerebral metabolic rate of oxygen at different values of SAR.

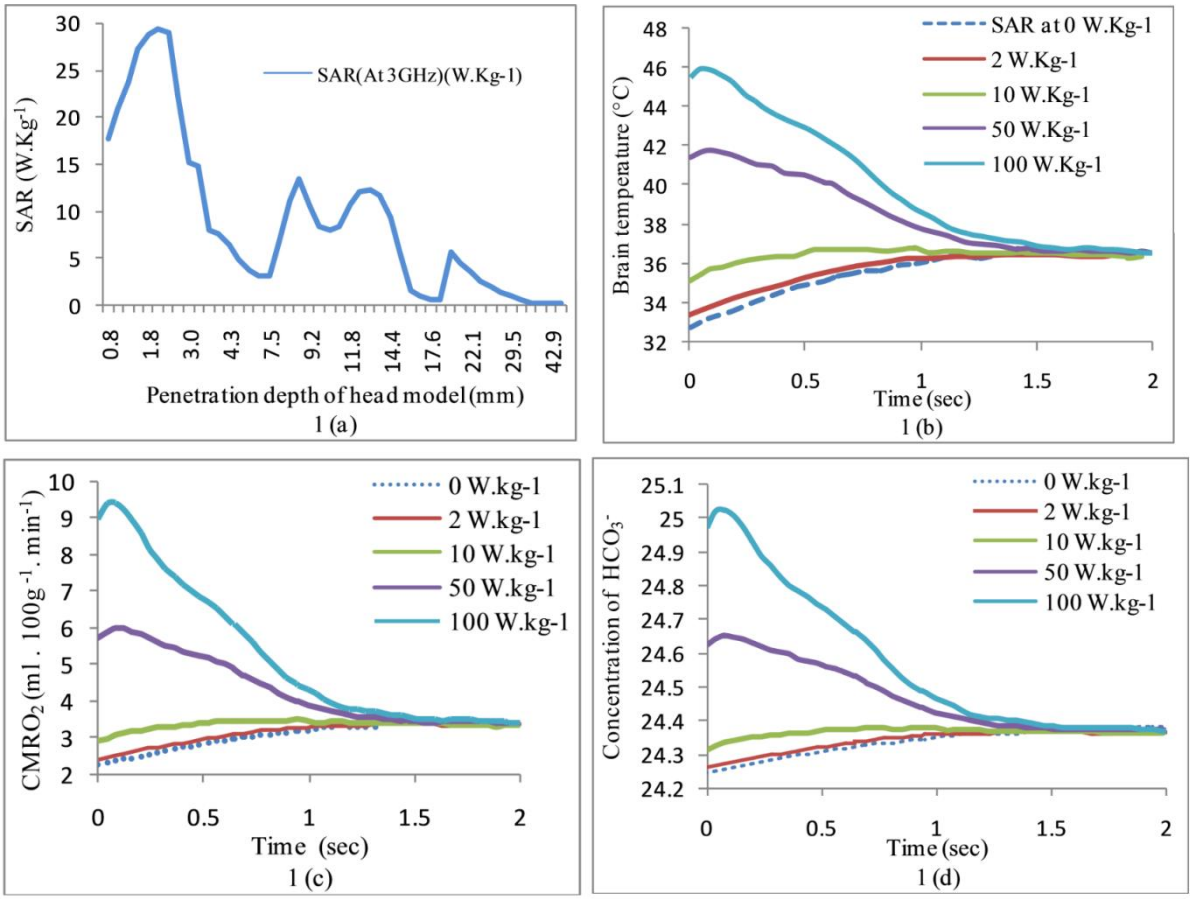

Figure 2: Simulation setup for intracranial dynamics (all abbreviations have been discussed in Table I.).

The concentration of released bicarbonate ions in blood plasma will increase the pressure of carbon dioxide in venous. The model calculates the increased concentration of bicarbonate ions in addition to its initial amount in the blood plasma as shown in Figure 1d. The relationship between bicarbonate ion concentration and CO_2 pressure is shown in Eq. 5 as given by Henderson-Hasselbach. The same has been used in the model to calculate the CO_2 pressure in the venous. The coupling between carbon dioxide pressure and CBF will increase the CBF as well as cerebral blood volume (CBV). Elevation in CBV will compress the brain tissue and decrease the cranial subarachnoid space where the CSF is absorbed. The resultant decrease in cerebral intracranial space for CSF absorption will lead to increase the pressure. This pressure is called intracranial pressure (ICP). Hence, the increase in CBV will elevate the ICP. The finding directs to a highly concerning aspect that the risk of brain tissue damage could be greater for those patients who have poor intracranial compliance (elasticity). Here a fixed value of compliance has been considered while simulating the model.

The result shows that high RF energy is associated with an increased risk of ICP. If ICP >

20mmg (Kawoos, Meng & Tofighi, 2015), patients require immediate care to control the ICP. Our idea is that the exposure of RF energy would result in an elevation of ICP which will have a harsh effect on persons with poor intracranial compliance. This finding indicates that the impact of increased ICP due to exposure of RF energy is influenced by compliance, although the real effect may have individual variations. Further investigations are required to clarify to what extent compliance determines the ICP response underexposure of RF energy.

The limitation of the model lies in its inability to simulate the concept of blood auto-regulation. Secondly, the exposure time of RF energy plays a significant role to increase the brain temperature and model does not address this factor.

VI. CONCLUSION

The major finding of this Simulation Model is that elevation in brain temperature under the exposure of RF energy is affecting the cerebral metabolic rate of oxygen, CBF, CBV and intracranial pressure. The motive behind this model is to improve the comprehension of ICP.

But these results are not extensive in general, it may have individual variations. This model offers a straight forward approach of bringing together the relationship between intracranial pressure and exposed RF energy. Some factors such as duration of exposure and cerebral blood auto-regulation have not been significantly addressed in this paper. Finally, this is asserted that the effect of RF energy on ICP, cerebral metabolism, and other parameters may not always be the same for every person. It may vary from person toperson. Further investigations are needed to obtain better guidelines to remove the health hazards from RF energy as per the individualized approach.

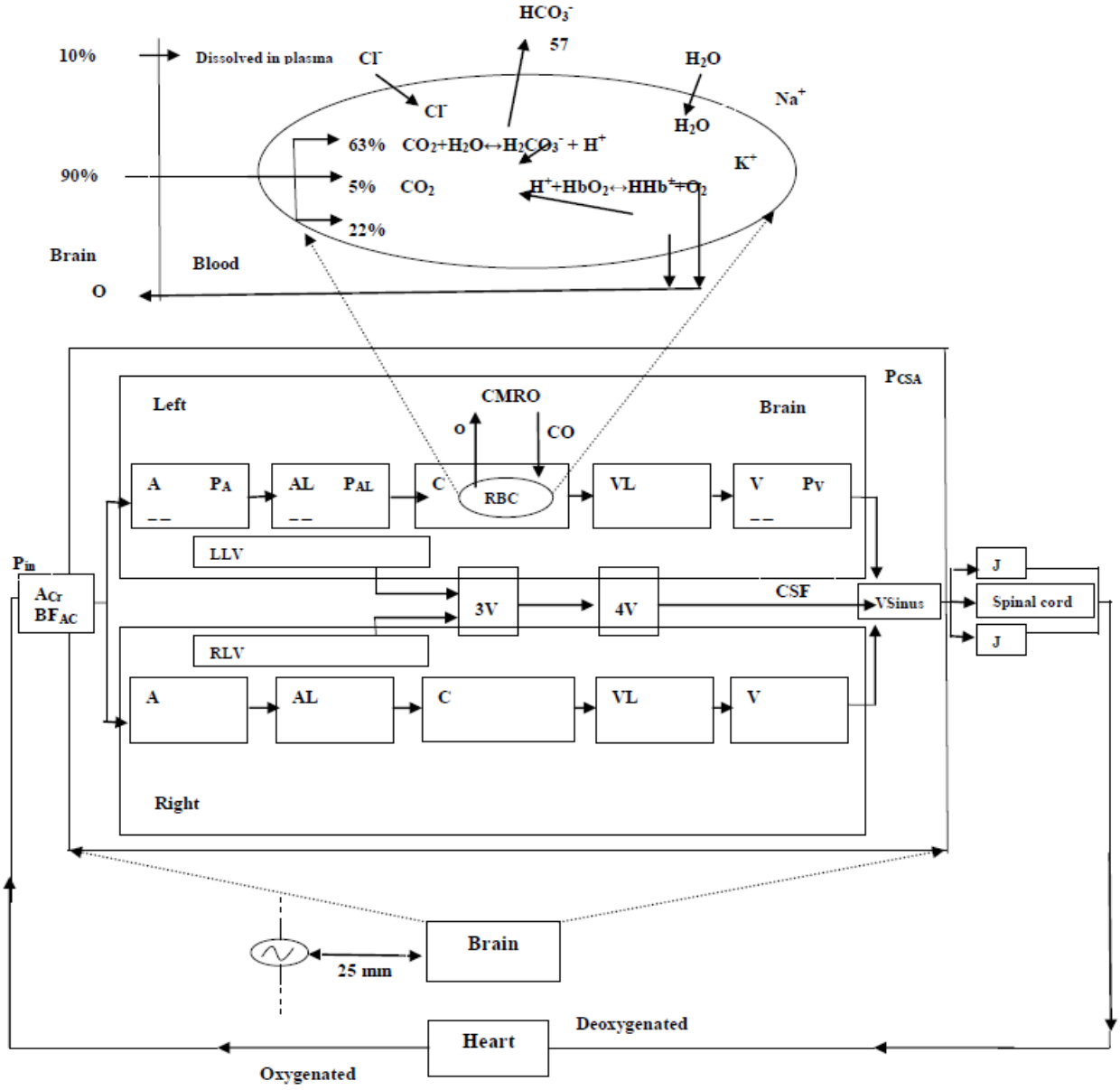

Figure 3: (a) plot shows Cardiac cycle for two seconds, (b) plot shows the blood flow (ml.min^{-1}) in carotid artery (A_{Cr}) for 200% cardiac cycle (100% cardiac cycle = 1 cardiac cycle), (c) plot represents the initial pressure (mmHg) in the carotid artery (P_{init}), pressure in artery (P_A), pressure in arterioles (P_{AL}), pressure in cranial subarachnoid space (P_{CSAS}), and pressure in vein (P_V) for two cardiac cycles, and (d) plot represents the initial blood flow (ml.sec^{-1}) in the artery (BF_A), blood flow in arterioles (BF_{AL}), and blood flow in venous (BF_V) as well as present an amount of cerebrospinal fluid (CSF) for two cardiac cycles.

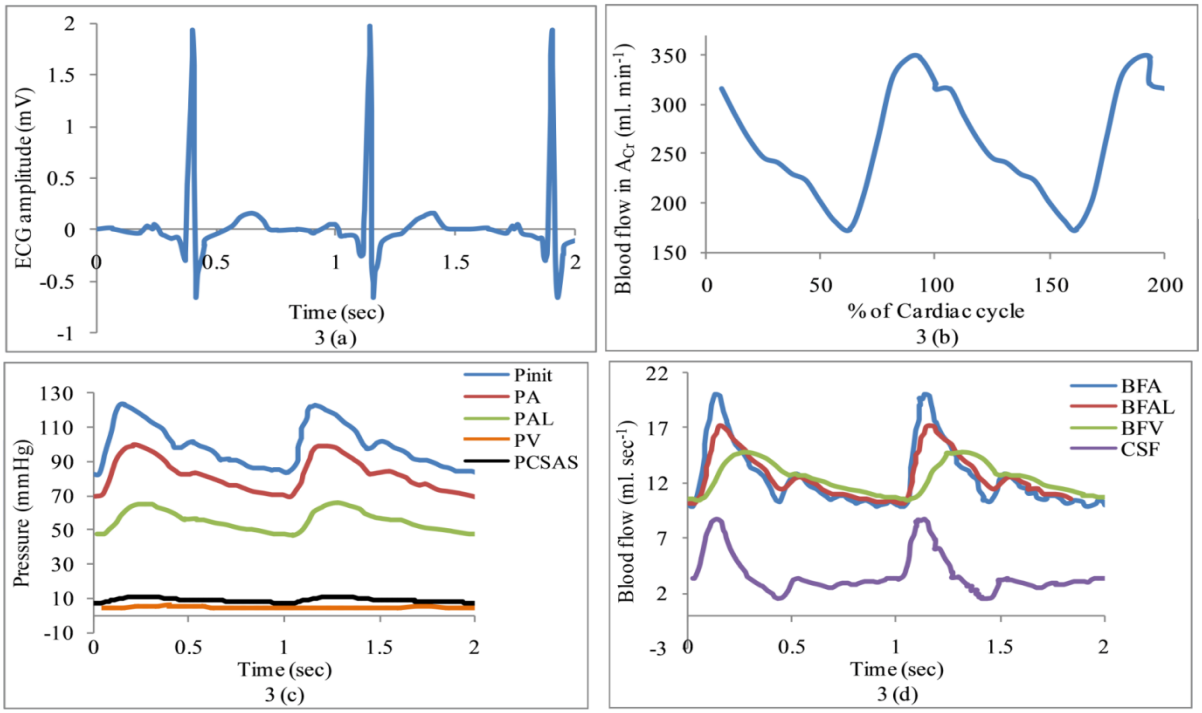

Figure 4: (a) plot shows the changes in cerebral blood volume (CBV) (ml.sec^{-1}) on different SAR values, (b) plot represents intracranial pressure is increased with an increase in SAR during exposure of RF energy.

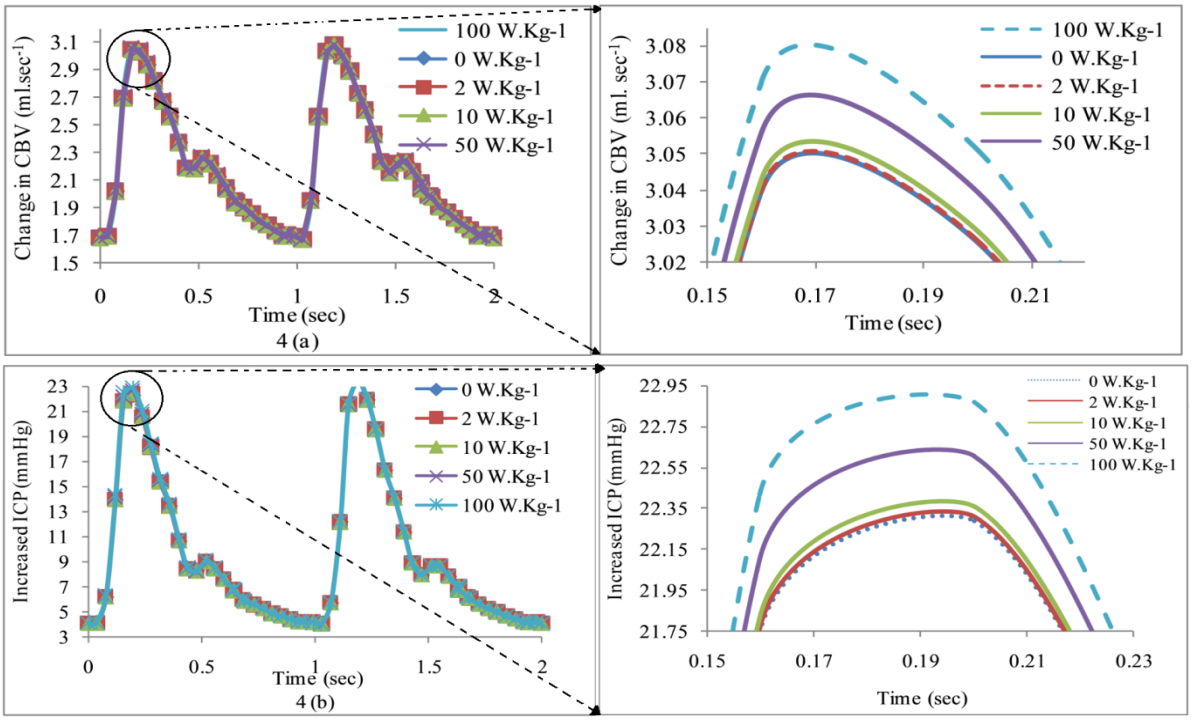

Figure 5: With an increase in brain temperature and SAR, ICP increases

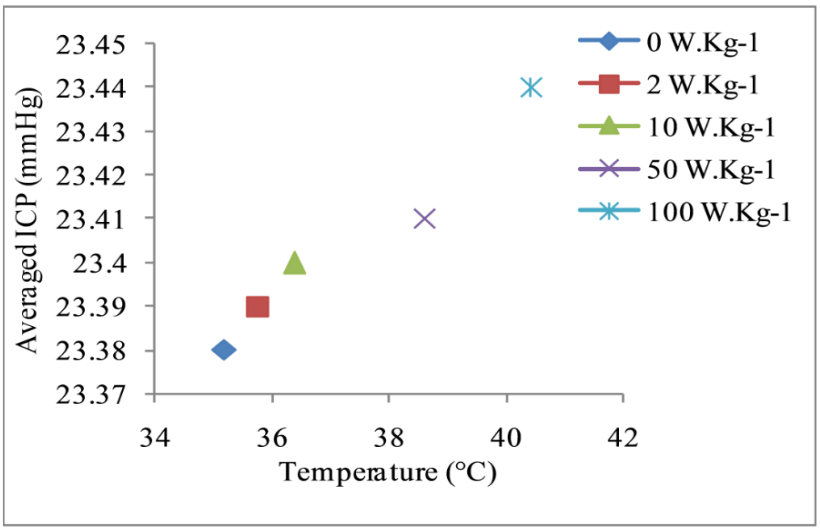

Table I. Definition of Abbreviations

Abbreviation	Interpretation	Abbreviation	Interpretation
A_{Cr}	Carotid artery	$P_{init.}$	Initial pressure in carotid artery
A	Artery	P_A	Pressure in artery
AL	Arterioles	P_{AL}	Pressure in arterioles
C	Capillary	P_V	Pressure in vein
VL	Veinules	P_{CSAS}	Pressure in cranial subarachnoid space
V	Vein	BF_{ACr}	Blood flow in carotid artery
VSinus	Venous sinus	BF_A	Blood flow in artery
JV	Jugular vein	BF_{AL}	Blood flow in arterioles
CSAS	Cranial subarachnoid space	BF_V	Blood flow in vein
CSF	Cerebrospinal fluid	$CMRO_2$	Cerebral metabolic rate of oxygen
LLV	Left lateral ventricle	BT	Brain temperature
RLV	Right lateral ventricle	$O_2\_C\_B_{tissue}$	Consumed O2 by brain tissue
3V	Third ventricle	$P\_CO_2\_B_{tissue}$	Produced CO2 by brain tissue
4V	Fourth ventricle	$[HCO_3^-]$	Concentration of bicarbonate ions
PCO_2	Carbon dioxide pressure	$PvCO_2$	CO2 pressure in venous

Retrieval Number: E6436018520/2020©BEIESP
DOI:10.35940/ijrte.E6436.018520
Journal Website: www.ijrte.org

Published By:
Blue Eyes Intelligence Engineering
& Sciences Publication

ICP (0)	Initial intracranial pressure	CBF	Cerebral blood flow
ICP(t)	Intracranial pressure at time t	CBV	Cerebral blood volume
SAR	Specific absorption rate	HbO_2	Oxygenated blood
RF	Radio frequency	ICH	Intracranial hypertension
K_e	Elasticity of blood vessel	ΔV	Change in cerebral volume due to blood and CSF

Table II: Percentage change in $CMRO_2$ at maximum brain temperature and different SAR values

Maximum Brain temperature (°C)	SAR (W/Kg)	$CMRO_2$ (ml/100 g/min)	Steady state condition	Percentage change in $CMRO_2$
32.74	0	2.2	37°C	34.1 ↓
33.34	2	2.3		34.3 ↓
35.13	10	2.8		20 ↓
41.39	50	5.7		64 ↑
45.50	100	8.9		150 ↑

↓- decreasing the value of corresponding parameter
↑- increasing the value of corresponding parameter

REFERENCES

1. Akdag, M., Dasdag, S., Canturk, F., Akdag, M. Z. (2018). Exposure to non-ionizing electromagnetic fields emitted from mobile phones induced DNA damage in human ear canal hair follicle cells. Electromagnet. Biol. Med. 37:66–75. doi 10.1080/15368378.2018.1463246
2. Akdag, M. Z., Dasdag, S., Canturk, F., et al. (2016). Does prolonged radiofrequency radiation emitted from Wi-Fi devices induce DNA damage in various tissues of rats? J. Chem. Neuroanat. 75:116–122. doi 10.1016/j. jchemneu.2016.01.003.
3. Arthurs, G. J., Sudhakar, M. (2005). Carbon dioxide transport. Continuing Education in Anaesthesia Critical Care & Pain, 5(6), 207–210. doi 10.1093/bjaceaccp/mki050
4. Belyaev, A. (2012). Evidence for disruption by modulation role of physical and biological variables in bioeffects of non-thermal microwaves for reproducibility, cancer risk and safety standards. In: Sage, C., Carpenter, D. (eds.), Bioinitiative Working Group, Section 15. Bioinitiative Report WHO 2012. WHO Press: Switzerland. pp. 1–71.
5. Cam, S. T., Seyhan, N. (2012). Single-strand DNA breaks in human hair root cells exposed to mobile phone radiation. Int. J. Radiat. Biol. 88:420–424. doi 10.3109/ 09553002.2012.666005.
6. Chauhana, P., Verma, H. N., Sisodia, R., Kesari, K. K. (2017). Microwave radiation (2.45 GHz)-induced oxidative stress: Whole-body exposure effect on histopathology of wistar rats. Electromagn. Biol. Med. 36:20–30. doi 10.3109/15368378.2016.1144063
7. Croughwell, N. D., Smith, L. R., Quill, T. J., Newman, M. F., Greeley, W. J., Kern, F., Lu, J., Reves, J. G. (1992). The effect of temperature on cerebral metabolism and blood flow in adults during cardiopulmonary bypass. Journal of Thoracic and Cardiovascular Surgery, 103(3), 549-554.
8. Dasdag, S., Akdag, M. Z., Erdal, M. E., et al.. (2015). Effects of 2.4 GHz radiofrequency radiation emitted from Wi-Fi equipment on microRNA expression in brain tissue. Int. J. Radiat. Biol. 91(7):555–561. doi 10.3109/ 09553002.2015.1028599.
9. Deshmuck, P. S., Megha, K., Banerjee, B. D., et al. (2013). Detection of low level microwave radiation induced deoxyribonucleic acid damage vis-a-vis genotoxicity in brain of Fischer rats. Toxicol. Int. 20:19–24. doi 10.4103/09716580.111549.
10. Edvinsson, L., Mackenzie, E. T., McCulloch, J. (1993). Cerebral Blood Flow and Metabolism. Journal of Neurochemistry, 62(2), pp. 683. doi 10.1046/j.1471-4159.1994.62020819.x
11. Fleisher, G. R., Ludwig, S., Silverman, B. K. (2002). Synopsis of Pediatric Emergency Medicine. (4th ed.), Philadelphia, PA: Lippincott Williams and Wilkins.
12. Ganong, W. F. (1995). Review of Medical Physiology. (17th ed.), Buckley, UK: Connecticut: Appleton & Lange.
13. Geers, C., Gros, G. (2000). Carbon Dioxide Transport and Carbonic Anhydrase in Blood and Muscle. Physiological Reviews, 80(2), 681-715. doi 10.1152/physrev.2000.80.2.681
14. Geocadin, R. G., Varelas, P. N., Rigamonti, D., Williams, M. A. (2007). Continuous intracranial pressure monitoring via the shunt reservoir to assess suspected shunt malfunction in adults with hydrocephalus. Neurosurgical Focus, 22(4), E10. doi 10.3171/foc.2007.22.4.12
15. Gowers, W. R. (1886). A Manual of Diseases of the Nervous System. London: J. & A. Churchill.

16. Goyal, K., Uddin, M., Salwan, S. K. (2017). Modeling and Simulation Study of Cerebrospinal Fluid Circulation in Human Brain. IEEE 4th International Conference on Signal Processing and Integrated Networks (SPIN), India, pp. 104-108. doi 10.1109/SPIN.2017.8049925.
17. Greeley, W. J., Kern, F. H., Ungerleider, R. M., Boyd, J. L. III., Quill, T., Smith, L. R., Baldwin, B., Reves, J. G. (1991). The effect of hypothermic cardiopulmonary bypass and total circulatory arrest on cerebral metabolism in neonates, infants, and children. J Thorac Cardiovasc Surg., 101(5), 783-794
18. Grubbjr, R. L., Raichle, M. E., Eichling, J. O., Ter-Pogossian, M. M. (1974). The effects of Changes in PaCO2 on Cerebral, Blood Volume, Blood Flow, and Vascular Mean Transit Time. Stroke, 5(5), 630-639. doi 10.1161/01.STR.5.5.630
19. Hamani, C., Zanetti, M. V., Pinto, F. C., Andrade, A. F., Ciquini, O. Jr., Marino, R. Jr. (2003). Intraventricular pressure monitoring in patients with thalamic and ganglionic haemorrhages. Arq NeuroPsiquiatr., 61(2B), 376-380. doi 10.1590/S0004-282X2003000300010
20. Hardell, L., Carlberg, M. (2009). Mobile phones, cordless phones and the risk for brain tumours. Int. J. Oncol. 35(1):5–17. doi 10.3892/ijo_00000307
21. Higgins, C. (2008). Parameters that reflect the carbon dioxide content of blood. pp: 959-961. Retrieved from: https://acutecaretesting.org//media/acutecaretesting/files/pdf/parameters-that-reflect-the-carbon-dioxide-content-of-blood.pdf
22. ICNIRP Guidelines. (1998). For limiting exposure to time-varying electric, magnetic, and electromagnetic fields (up to 300 GHz). Health Physics Society, 74(4), 494-522. https://www.icnirp.org/cms/upload/publications/ICNIRPemfgdl.pdf
23. Kawoos, U., Meng, Xu., Tofighi, M. R. (2015). Too Much Pressure: Wireless Intracranial Pressure Monitoring and Its Application in Traumatic Brain Injuries. IEEE Microwave Magazine, pp: 39-53. doi 10.1109/MMM.2014.2377585
24. Kodera, S., Tames, J. G., Hirata, A. (2018). Temperature elevation in the human brain and skin with thermoregulation during exposure to RF energy. BioMedical Engineering OnLine, 17, 1-17. doi 10.1186/s12938-017-0432-x
25. Linninger, A. A., Xenos, M., Sweetman, B., Ponkshe, S., Guo, X., Penn, R. (2009). A mathematical model of blood, cerebrospinal fluid and brain dynamics. Journal of Mathematical Biology, 59(6), 729-759. doi 10.1007/s00285-009-0250-2
26. Lumb, A. (2012). Nunn's Applied Respiratory Physiology, Chapter 10, (7th ed.), Churchill Livingstone: Elsevier. **eBook ISBN:** 9780702054167
27. Megha, K., Deshmukh, P. S., Banerjee, B. D., et al. (2015). Low intensity microwave radiation induced oxidative stress, inflammatory response and DNA damage in rat brain. NeuroToxicology. 51:158–165. doi 10.1016/j. neuro.2015.10.009.
28. Mishra, L. D. (2002). Cerebral Blood Flow and Anaesthesia: A Review, Indian J. Anaesth., 46(2), 87-95. http://medind.nic.in/iad/t02/i2/iadt02i2p87.pdf
29. Mokri, B. (2001). The Monro-Kellie hypothesis: applications in CSF volume depletion. Neurology, 56(12), 1746-1748. doi 10.1212/WNL.56.12.1746
30. Nagaoka, T., Watanabe, S., Sakurai, K., Kunieda, E., Watanabe, S., Taki, M., Yamanaka, Y. (2004). Development of realistic high-resolution whole-body voxel models of Japanese adult males and females of average height and weight, and application of models to radio-frequency electromagnetic-field dosimetry. Physics in Medicine and Biology, 49(1), 1-15. doi 10.1088/0031-9155/49/1/001
31. Nittby, H., Grafström, G., Eberhardt, J. L., et al. (2008). Radiofrequency and Extremely Low-Frequency Electromagnetic Field Effects on the Blood-Brain Barrier. Journal of Electromagnetic Biology and Medicine, 27: 103-126. doi 10.1080/15368370802061995.
32. Nyholm, L., Howells, T., Lewén, A., Hillered, L., Enblad, P. (2017). The influence of hyperthermia on intracranial pressure, cerebral oximetry and cerebral metabolism in traumatic brain injury. Upsala Journal of Medical Sciences, 122(3), 177-184. doi 10.1080/03009734.2017.1319440
33. Pennes, H. H. (1948). Analysis of tissue and arterial blood temperatures in the resting human forearm. Journal of Applied Physiology, 1(2), 93–122. doi 10.1152/jappl.1948.1.2.93
34. Petersen, K. D., Landsfeldt, U., Cold, G. E., Petersen, C. B., Mau, S., Hauerberg, J., Holst, P., Olsen, K. S. (2003). Intracranial pressure and cerebral hemodynamic in patients with cerebral tumors: a randomized prospective study of patients subjected to craniotomy in propofol-fentanyl, isoflurane-fentanyl, or sevoflurane-fentanyl anesthesia. Anesthesiology, 98(2), 329-336. doi 0000542-200302000-00010
35. Taflove, A., & Hagness, S. C. (2005). *Computational Electrodynamics: The Finite-Difference Time-Domain Method*. (3rd ed.) Norwood, MA: Artech House.
36. Tameem, A., Krovvidi, H. (2013). Cerebral Physiology. Continuing Education in Anaesthesia Critical Care & Pain, 13(4), 113-118. doi 10.1093/bjaceaccp
37. Thoman, W. J., Lampotang, S., Gravenstein, D., Aa, J. V. D. (1997). A Computer Model of Intracranial Dynamics, 19th Annual International Conference-IEEE/EMBS, pp. 2197-2200, Chicago, IL. USA. doi 10.1109/IEMBS.1997.758793
38. WANG, C. Y., JU, Y., Li, X. Y. (2010). Study on Dynamics Modeling and Simulation of Cerebrospinal Fluid Circulation. IEEE 2nd International Conference on Information Sciences and Engineering, 610-613. doi 10.1109/ICISE.2010.5689951
39. Ziljstra WG, Cerebral blood flow, Basic knowledge and clinical implications, Vol. 7, Amsterdam: Excerpta Medica; 1981.

AUTHORS PROFILE

Kavita Goyal is pursuing her doctorate in Electronics and Communication Engineering from Apeejay Stya University, Sohna-Palwal Road, Gurugram, India. She did her BTech from Punjab Technical University, Jalandhar, India. She did her MTech from Apeejay College of Engineering under Maharishi Dayanand University, Rohtak, Haryana, India. She had experience in teaching of ten years. Her research interest includes bio-medical signal processing, brain- computer interface, embedded system. She has published more than 15 research papers in international journals, national and international conferences. She has coordinated various academic and administrative activities. She has organized many national level workshops and conferences. She is an eminent researcher.

Moin Uddin is working as Professor in Engineering & Technology at Apeejay Stya University, Sohna-Palwal Road, Gurugram, India. He has worked as Director, Dr. B. R. Ambedkar National Institute of Technology, Jalandhar, Punjab, India. He did his Doctorate in the field of Electronics & Computer Engineering, University of Roorkee, Roorkee (U.P), India. He has also worked as Pro Vice Chancellor of Delhi Technical University, India. He has vast knowledge and experience in the field of bio-medical instrumentation and analysis. He has been honored with Dr. S. RADHA KRISNAN award. He has many papers in National and International Journals to his credit and has guided many research scholars.